SCIENTIFIC REPORTS

OPEN

SUBJECT AREAS:
NANOPHOTONICS AND PLASMONICS
RENEWABLE ENERGY
SOLAR CELLS
SOLAR ENERGY AND PHOTOVOLTAIC TECHNOLOGY

Received
10 September 2013

Accepted
18 October 2013

Published
4 November 2013

Correspondence and requests for materials should be addressed to H.W.H. (hongwei.han@mail.hust.edu.cn)

Full Printable Processed Mesoscopic $CH_3NH_3PbI_3/TiO_2$ Heterojunction Solar Cells with Carbon Counter Electrode

Zhiliang Ku, Yaoguang Rong, Mi Xu, Tongfa Liu & Hongwei Han

Michael Grätzel Center for Mesoscopic Solar Cells, Wuhan National Laboratory for Optoelectronics, School of Optical and Electronic Information, Huazhong University of Science and Technology, Wuhan, Hubei 430074, P. R. China.

A mesoscopic methylammonium lead iodide ($CH_3NH_3PbI_3$) perovskite/TiO_2 heterojunction solar cell is developed with low-cost carbon counter electrode (CE) and full printable process. With carbon black/spheroidal graphite CE, this mesoscopic heterojunction solar cell presents high stability and power conversion efficiency of 6.64%, which is higher than that of the flaky graphite based device and comparable to the conventional Au version.

Photovoltaic has been realized as a suitable generating electrical power by converting solar radiation into direct current electricity for the fulfillment of increasing world energy consumption with the least impact on the environment. Although solid state junction devices with high efficiency, usually made of silicon and compound semiconductors, dominate the commercial market, these photovoltaic technologies still receive constraints in market development due to both of expensive materials and complex manufacturing processes[1–4]. Consequently, the emerging photovoltaic technologies such as organic cells[5–7], inorganic cells[8,9], quantum dot cells[3] and dye-sensitized solar cells (DSSCs)[1,2,10–13], have attracted extensive attention because of their promising inexpensive techniques based on the solution-processed materials. However, these emerging photovoltaic technologies seem to be always associated with unsatisfactory efficiency.

In the past two years, methylammonium lead halide ($CH_3NH_3PbX_3$, X = I, Cl or Br) and its mixed-halide crystals, corresponding to three-dimensional perovskite structures, have been used as light harvesters for mesoscopic heterojunction solar cells[14]. The advantages of the direct band gap, large absorption coefficient, and high carrier mobility of methylammonium lead halide perovskite nanocrystals render them to be perfect light harvesters[15–17]. Most recently, a high efficiency about 12 ~ 15%, which is comparable to that of the commercial silicon solar cells, has been achieved in solid-state mesoscopic solar cells employing organic hole transporting materials such as Spiro-OMeTAD, PTAA and so on[18–25]. More importantly, these perovskite nanocrystals can be synthesized by simple and cheap techniques due to their self-assembling character, implying a great potential to bring down the cost of energy production. However, the counter electrodes (CEs) of these high performance photovoltaic devices still need noble mental such as Au or Ag, prepared by thermal evaporation under high vacuum condition[15,18,19]. Obviously, this high-cost metallic CE is an issue for its large-scale production. Meanwhile, the vacuum evaporation process is also highly energy consumptive and draws apart from its promising inexpensive techniques[1]. Therefore, the replacement of the costly metallic CEs would be a critical improvement for this kind of high-efficiency heterojunction photovoltaic cells based on $CH_3NH_3PbI_3$ nanocrystalline light harvester.

Carbon is an abundantly available and low-cost material, which have been applied in DSSCs successfully[26–29]. In 1996, Kay and Grätzel firstly reported a new type of liquid monolithic DSSC employing carbon black/graphite composite CE and obtained a promising *PCE* of 6.7%[26]. This monolithic photovoltaic device permits printing paste layer by layer on a single FTO glass substrate by screen-printing technique, which offers more positive prospect for commercial production. Moreover, the work function of carbon (−5.0 eV) is close to Au (−5.1 eV). Although these advantages indicate that carbon may be an ideal material to substitute Au as a CE in $CH_3NH_3PbI_3$ heterojunction photovoltaic cells, to date, none relevant research has been reported. In this communication, we assemble a monolithic $CH_3NH_3PbI_3$ perovskite/TiO_2 heterojunction solar cell based on Carbon black/Graphite CE and printable process. Due to the $CH_3NH_3PbI_3$ perovskite be capable of acting as a light harvester and at the same time as a hole conductor[15], herein we fabricate such heterojunction photovoltaic device without any organic p-type material for transporting positive charge carrier. The results indicates that the mesoscopic heterojunction

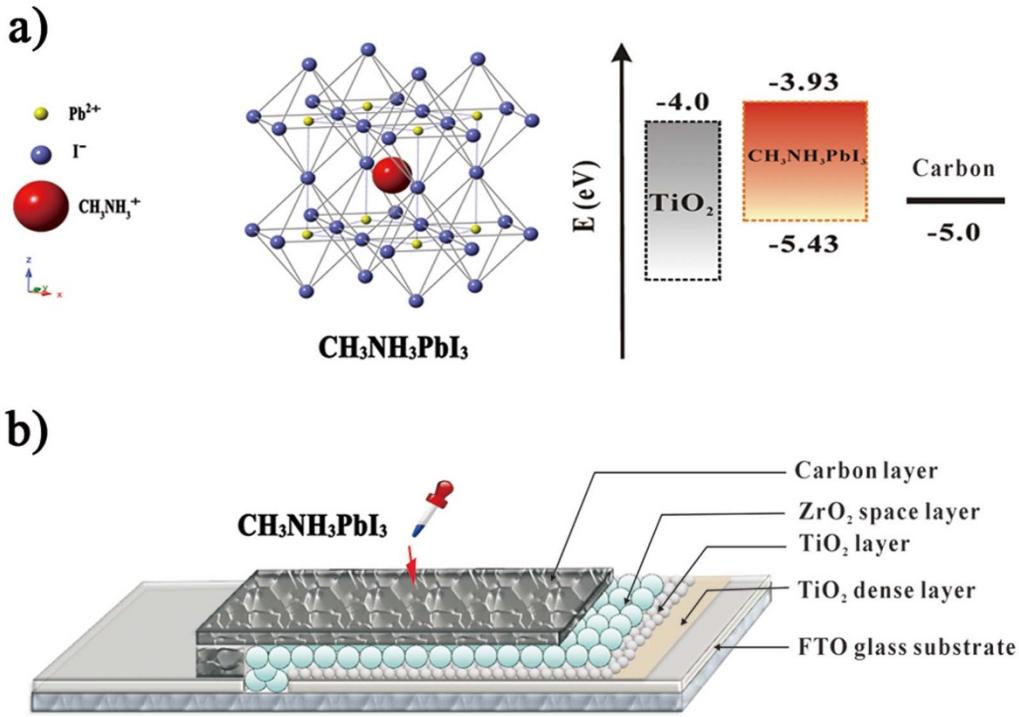

Figure 1 | (a) The crystal structure of $CH_3NH_3PbI_3$ perovskite and the corresponding energy levels of TiO_2, $CH_3NH_3PbI_3$, and Carbon. (b) A schematic structure of a carbon based monolithic device.

solar cell with carbon black/spheroidal graphite counter electrode presents high stability and power conversion efficiency of 6.64%, which is higher than those of the flaky graphite based device and comparable to the conventional Au version.

Results

$CH_3NH_3PbI_3$ has a perovskite structure, as shown in Figure 1a, which is composited of one Pb^{2+}, one CH_3NH^{3+}, and three iodine anions in the unit cell. Hence, we prepared lead iodide perovskite precursor solution by mixing the CH_3NH_3I and PbI_2 at 1 : 1 molar ratio to meet the atom ratio in $CH_3NH_3PbI_3$. In the manufacturing steps of carbon black/graphite based monolithic device (see Figure 1b), the FTO glass substrates were firstly etched with a laser to form two detached electrode patterns before being cleaned ultrasonically with ethanol. Then, the patterned substrates were coated by a TiO_2 dense layer by aerosol spray pyrolysis, and a 1 μm nanoporous TiO_2 layer was deposited by screen printing with the TiO_2 slurry (PASOL HPW-18NR). After being sintered at 450°C for 30 min, a 1 μm ZrO_2 space layer was printed on the top of the nanoporous TiO_2 layer using a ZrO_2 paste, which acts as a insulating layer to prevent short circuit. Finally, a carbon black/graphite CE was coated on the top of ZrO_2 layer by printing carbon black/graphite composite slurry and sintering at 400°C for 30 min. After optimization (see Figure S1 ESI†), the thickness of carbon black/graphite CE was controlled to about 10 μm.

The synthesis of $CH_3NH_3PbI_3$ and deposition on the monolithic device was carried out by drop-coating of a 30 wt% precursor solution onto the carbon black/graphite layer. Upon drying at 50°C, the films darkened in color, indicating the formation of $CH_3NH_3PbI_3$ in the solid state, confirmed by X ray diffraction (XRD) spectroscopy (see Figure S2, ESI†). In our device, when the $CH_3NH_3PbI_3$ absorbing light, it generate electron on the conduction band (−3.93 eV) and hole on the valence band (−5.43 eV). Since the conduction band of TiO_2 is at −4.0 eV and the conduction band of ZrO_2 is at −3.27 eV, the electron on $CH_3NH_3PbI_3$ conduction band could only inject into TiO_2. Meanwhile, the hole on $CH_3NH_3PbI_3$ valence band could inject into the carbon (−5.0 eV) (see Figure 1a). Under AM1.5 solar

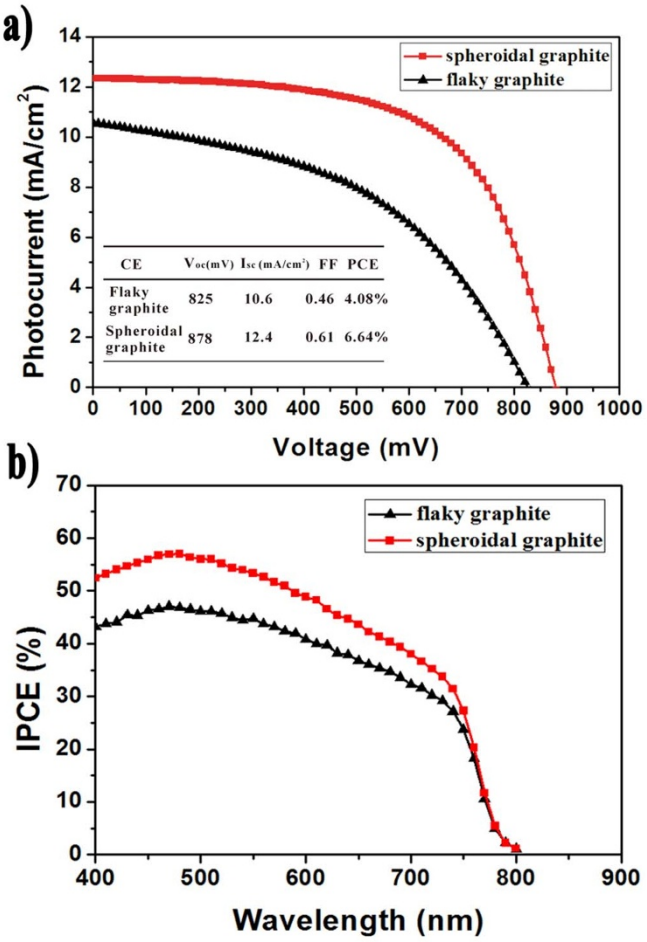

Figure 2 | (a) Photovoltaic characteristics of $CH_3NH_3PbI_3$ perovskite/TiO_2 heterojunction solar cell based different carbon CEs. (b) IPCE as function of incident wavelength.

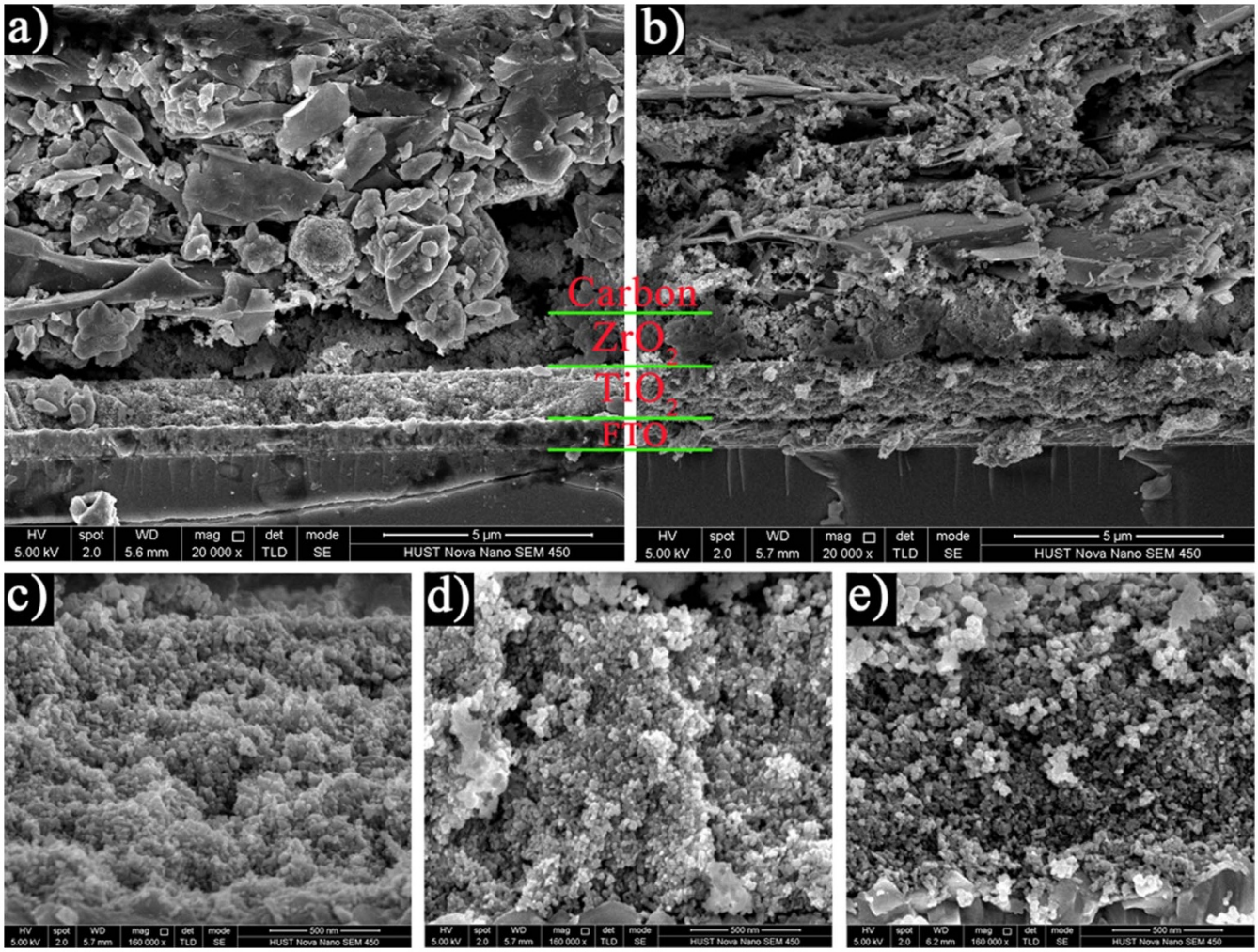

Figure 3 | Cross-sectional structure of the devices. (a) Spheroidal graphite (SG) based monolithic device. (b) Flaky graphite (FG) based monolithic device. (c) $CH_3NH_3PbI_3$ coated SG-TiO_2 film. (d) $CH_3NH_3PbI_3$ coated FG-TiO_2 film. (e) Bare TiO_2 film.

light of 100 mW·cm^{-2}, the carbon black/flaky graphite based monolithic device produced V_{oc} = 0.825 V and J_{sc} = 10.6 mA·cm^{-2}, with *FF* = 0.46, corresponding to a *PCE* of 4.08%. For further improving the device performance, spheroidal graphite with better conductivity (see Table S1, ESI†) and favorable morphology for pore-filling was used in the carbon composite CE to replace the flaky graphite. It could be found that the spheroidal graphite based device showed a much higher performance (V_{oc} = 0.878 V, J_{sc} = 12.4 mA·cm^{-2}, *FF* = 0.61, and a *PCE* of 6.64%) than that of the flaky graphite based device (See Figure 2a). The superiority of spheroidal graphite in device performance could be confirmed by the statistical data showed in Figure S3 and Table S2. These results indicate that the spheroidal graphite CE possess a potential capacity to replacing Au CE[15].

The incident photo to current conversion efficiency (IPCE) specifies the ratio of extracted electrons to incident photons at a given wavelength, which reflects the light response of the devices and is directly related to the J_{sc}. From the IPCE spectrum in Figure 2b, we can observe an excellent photocurrent response from 400 to 800 nm showed by the $CH_3NH_3PbI_3/TiO_2$ heterojunction devices. Moreover, the IPCE of spheroidal graphite based device reached a higher value than the flaky graphite based device in the full-scale visible region of the electromagnetic spectrum, in reasonable agreement with the measured values of *J-V* curves.

In order to investigate the huge difference in device performance of the two kinds of graphite based CEs, scanning electron microscopy (SEM) images have been observed from the cross section of the monolithic devices. Figure 3a and b show the different morphology of the spheroidal graphite and flaky graphite layers in monolithic devices. It' evident that spheroidal graphite possess a loose structure, attribute to the spheroidal morphology. However, in the flaky graphite based CE, large graphite sheets are stacked on the top of ZrO_2 space layer. In view of the fact that the devices fabricated by spheroidal graphite perform much higher *FF* than the ones fabricated by flaky graphite, which deduce a better pore-filling in the TiO_2 films of spheroidal graphite based monolithic devices. To confirm it, amplified SEM images of the cross section of TiO_2 films have been obtained. From these images, we can find both of the TiO_2 films in spheroidal graphite (SG-TiO_2, Figure 3c) and flaky graphite (FG-TiO_2, Figure 3d) based devices are coated by $CH_3NH_3PbI_3$ apparently, compared to the bare TiO_2 film (Figure 3e). It's notable that the $CH_3NH_3PbI_3$ coated on SG-TiO_2 are more uniform than that on FG-TiO_2, corresponding a higher *FF* in spheroidal graphite based device. We impute the uneven distribution of $CH_3NH_3PbI_3$ in FG-TiO_2 to the arrangement style of flaky graphite, since the perovskite $CH_3NH_3PbI_3$ coating on TiO_2 surface prepared by drop-coating precursor solution onto the carbon black/graphite layer.

Finally, the long-term stability in the dark of the carbon black based monolithic $CH_3NH_3PbI_3$ perovskite/TiO_2 heterojunction solar cells with the initial efficiency of 6.64% was tested under conditions stored in dry air at room temperature without encapsulation and presented in Figure 4. It could be found that after 840 hours,

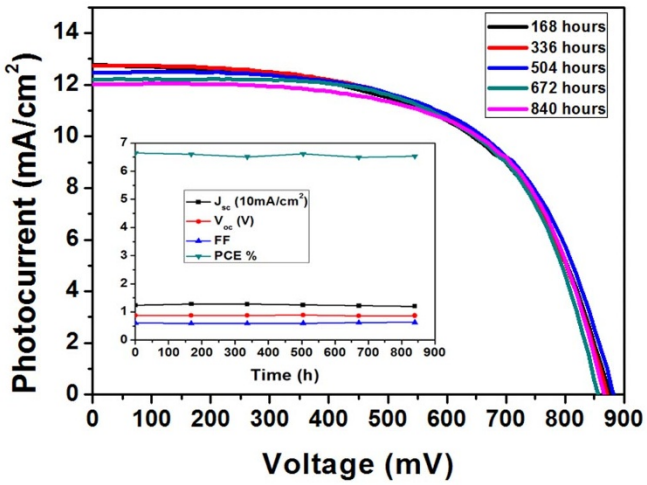

Figure 4 | Long term stability at room temperature in the dark. Inset: the changing characters of the device in 840 h after been fabricated.

although a slight decrease of J_{sc} was measured, the *PCE* value still remained above 6.5%. These impressive results are indicative of the superior stability of the $CH_3NH_3PbI_3$ perovskite/TiO_2 heterojunction devices.

Discussion

The present work established for the first time that carbon black/graphite can substitute noble metallic materials as an efficient CE in the application of hole-conductor-free $CH_3NH_3PbI_3$ perovskite/TiO_2 heterojunction solar cells. Impressive *PCE* values of exceeding 6.64% have been obtained with $CH_3NH_3PbI_3/TiO_2$ heterojunction device based on carbon black/spheroidal graphite CE. There still remains room for further greatly substantial improvement in the *PCE*, in particular by augmentation of the J_{sc} through control of the $CH_3NH_3PbI_3$ perovskite crystallinity and the interface engineering. The fact that carbon black/graphite CE can prepared by screen printing permits the commercial production of high-efficiency $CH_3NH_3PbI_3$ perovskite/TiO_2 heterojunction solar cells. Furthermore, the simple fabrication process and long-term stability of such kind of carbon/graphite based monolithic $CH_3NH_3PbI_3/TiO_2$ heterojunction devices open up new avenues for future development of low-cost photovoltaic cells.

Methods

Fabrication of mesoscopic $CH_3NH_3PbI_3/TiO_2$ heterojunction solar cells. FTO glass plates with high transparency in the visible range were etched with a laser to form two detached electrode pattern before being ultrasonically cleaned with detergent, deionized water and ethanol successively. After that, the patterned substrates were coated with a roughly 100 nm compact TiO_2 layer by aerosol spray pyrolysis at 450°C. After cooling down to room temperature naturally, a 1 μm TiO_2 nanocrystalline layer (PASOL HPW-18NR) was deposited on top of the compact layer by screen printing and then sintered at 500°C for 30 min. Followed, a 1 μm ZrO_2 spacer layer and a 10 μm mesoscopic carbon layer was printed on the top of the TiO_2 nanocrystalline layer successively, and then the films were sintered at 400°C for 30 min (See Figure S4 ESI†). After cooling down, 5 μL of the $CH_3NH_3PbI_3$ precursor (0.123 g CH_3NH_3I and 0.3625 g PbI_2 were mixed in 1 mL γ-butyrolactone) was dipped on the top of the mesoscopic carbon layer. Then the devices were dried at 50°C on a hot plate under dark. During the drying procedure, the coated devices changed color from light yellow to dark brown, indicating the accomplishment of the solar cell.

Characterization. The cross section of the devices and the carbon films were imaged by a field-emission scanning electron microscope (FE-SEM). Photocurrent density-voltage (*J-V*) characteristics were measured using a Keithley 2400 source/meter and a Newport solar simulator (model 91192-1000) giving light with AM 1.5 G spectral distribution. A black mask with a circular aperture (0.125 cm^2) smaller than the active area of the square solar cell (0.5 cm^2) was applied on top of the cell. The incident photon conversion efficiency (IPCE) was measured using a 150 W xenon lamp (Oriel) fitted with a monochromator (Cornerstone 74004) as a monochromatic light source.

1. Hardin, B. E., Snaith, H. J. & McGehee, M. D. The renaissance of dye-sensitized solar cells. *Nat. Photon.* **6**, 162–169 (2012).
2. Graetzel, M., Janssen, R. A. J., Mitzi, D. B. & Sargent, E. H. Materials interface engineering for solution-processed photovoltaics. *Nature* **488**, 304–312 (2012).
3. Sargent, E. H. Colloidal quantum dot solar cells. *Nat. Photon.* **6**, 133–135 (2012).
4. Blom, P. W. M., Mihailetchi, V. D., Koster, L. J. A. & Markov, D. E. Device Physics of Polymer:Fullerene Bulk Heterojunction Solar Cells. *Adv. Mater.* **19**, 1551–1566 (2007).
5. Scharber, M. C. *et al.* Design Rules for Donors in Bulk-Heterojunction Solar Cells–Towards 10% Energy-Conversion Efficiency. *Adv. Mater.* **18**, 789–794 (2006).
6. Leong, W. L., Cowan, S. R. & Heeger, A. J. Differential Resistance Analysis of Charge Carrier Losses in Organic Bulk Heterojunction Solar Cells: Observing the Transition from Bimolecular to Trap-Assisted Recombination and Quantifying the Order of Recombination. *Adv. Energy Mater.* **1**, 517–522 (2011).
7. Chen, L.-M., Hong, Z., Li, G. & Yang, Y. Recent Progress in Polymer Solar Cells: Manipulation of Polymer:Fullerene Morphology and the Formation of Efficient Inverted Polymer Solar Cells. *Adv. Mater.* **21**, 1434–1449 (2009).
8. Li, J. B., Chawla, V. & Clemens, B. M. Investigating the role of grain boundaries in CZTS and CZTSSe thin film solar cells with scanning probe microscopy. *Adv. Mater.* **24**, 720–723 (2012).
9. Singh, A., Geaney, H., Laffir, F. & Ryan, K. M. Colloidal synthesis of wurtzite Cu_2ZnSnS_4 nanorods and their perpendicular assembly. *J. Am. Chem. Soc.* **134**, 2910–2913 (2012).
10. Oregan, B. & Gratzel, M. A low-cost, high-efficiency solar cell based on dye-sensitized colloidal TiO_2 films. *Nature* **353**, 737–740 (1991).
11. Han, H. W., Liu, W., Zhang, J. & Zhao, X. Z. A hybrid poly(ethylene oxide)/poly(vinylidene fluoride)/TiO2 nanoparticle solid-state redox electrolyte for dye-sensitized nanocrystalline solar cells. *Adv. Funct. Mater.* **15**, 1940–1944 (2005).
12. Li, X. *et al.* Efficient Dye-Sensitized Solar Cells with Potential-Tunable Organic Sulfide Mediators and Graphene-Modified Carbon Counter Electrodes. *Adv. Funct. Mater.* **23**(26), 3344–3352 (2013).
13. Grätzel, C. & Zakeeruddin, S. M. Recent trends in mesoscopic solar cells based on molecular and nanopigment light harvesters. *Mater. Today* **16**, 11–18 (2013).
14. Noh, J. H., Im, S. H., Heo, J. H., Mandal, T. N. & Seok, S. I. Chemical Management for Colorful, Efficient, and Stable Inorganic–Organic Hybrid Nanostructured Solar Cells. *Nano Lett.* **13**, 1764–1769 (2013).
15. Etgar, L. *et al.* Mesoscopic $CH_3NH_3PbI_3/TiO_2$ Heterojunction Solar Cells. *J. Am. Chem. Soc.* **134**, 17396–17399 (2012).
16. Kojima, A., Ikegami, M., Teshima, K. & Miyasaka, T. Highly Luminescent Lead Bromide Perovskite Nanoparticles Synthesized with Porous Alumina Media. *Chem. Lett.* **41**, 397–399 (2012).
17. Kagan, C. R., Mitzi, D. B. & Dimitrakopoulos, C. D. Organic-Inorganic Hybrid Materials as Semiconducting Channels in Thin-Film Field-Effect Transistors. *Science* **286**, 945–947 (1999).
18. Burschka, J. *et al.* Sequential deposition as a route to high-performance perovskite-sensitized solar cells. *Nature* (2013).
19. Heo, J. H. *et al.* Efficient inorganic-organic hybrid heterojunction solar cells containing perovskite compound and polymeric hole conductors. *Nat. Photon.* **7**, 486–491 (2013).
20. Chen, H. *et al.* Efficient panchromatic inorganic-organic heterojunction solar cells with consecutive charge transport tunnels in hole transport material. *Chem. Commun.* **49**, 7277–7279 (2013).
21. Green, M. A., Emery, K., Hishikawa, Y., Warta, W. & Dunlop, E. D. Solar cell efficiency tables (version 39). *Prog. Photovol: Res. Appl.* **20**, 12–20 (2012).
22. Cai, B., Xing, Y., Yang, Z., Zhang, W.-H. & Qiu, J. High performance hybrid solar cells sensitized by organolead halide perovskites. *Energy Environ. Sci.* **6**, 1480–1485 (2013).
23. Ball, J. M., Lee, M. M., Hey, A. & Snaith, H. Low-Temperature Processed Mesosuperstructured to Thin-Film Perovskite Solar Cells. *Energy Environ. Sci.* **6**, 1739–1743 (2013).
24. Lee, M. M., Teuscher, J., Miyasaka, T., Murakami, T. N. & Snaith, H. J. Efficient Hybrid Solar Cells Based on Meso-Superstructured Organometal Halide Perovskites. *Science* **338**, 643–647 (2012).
25. Kojima, A., Teshima, K., Shirai, Y. & Miyasaka, T. Organometal Halide Perovskites as Visible-Light Sensitizers for Photovoltaic Cells. *J. Am. Chem. Soc.* **131**, 6050–6051 (2009).
26. Kay, A. & Grätzel, M. Low cost photovoltaic modules based on dye sensitized nanocrystalline titanium dioxide and carbon powder. *Sol. Energy Mate. Sol. Cells* **44**, 99–117 (1996).
27. Liu, G. H. *et al.* An efficient thiolate/disulfide redox couple based dye-sensitized solar cell with a graphene modified mesoscopic carbon counter electrode. *Carbon* **53**, 11–18 (2013).
28. Liu, G. H. *et al.* A mesoscopic platinized graphite/carbon black counter electrode for a highly efficient monolithic dye-sensitized solar cell. *Electrochim. Acta* **69**, 334–339 (2012).

29. Han, H. W., Bach, U., Cheng, Y. B., Caruso, R. A. & MacRae, C. A design for monolithic all-solid-state dye-sensitized solar cells with a platinized carbon counterelectrode. *Appl. Phys. Lett.* **94**, 103102 (2009).

Acknowledgments

The authors acknowledge the financial support from the Ministry of Science and Technology of China (863, No. SS2013AA50303), the National Natural Science Foundation of China (Grant No. 61106056), the Fundamental Research Funds for the Central Universities (HUSTNY022), and Scientific Research Foundation for Returned Scholars, Ministry of Education of China. We also thank the Analytical and Testing Center of Huazhong University of Science and Technology [HUST] for field emission scanning electron microscopy [FE-SEM] and X-ray diffraction (XRD) testing.

Author contributions

H.W.H. contributed to the conception and design of experiment, analysis of the data and write the manuscript with assistance of Z.L.K. Z.L.K. carried out the DSC studies, participated in the sequence alignment. Y.G.R., M.X. and T.F.L. participated in the materials preparation.

Additional information

Supplementary information accompanies this paper at http://www.nature.com/scientificreports

Competing financial interests: The authors declare no competing financial interests.

How to cite this article: Ku, Z., Rong, Y., Xu, M., Liu, T. & Han, H. Full Printable Processed Mesoscopic $CH_3NH_3PbI_3/TiO_2$ Heterojunction Solar Cells with Carbon Counter Electrode. *Sci. Rep.* **3**, 3132; DOI:10.1038/srep03132 (2013).